Biomed Microdevices (2015) 17: 108
DOI 10.1007/s10544-015-0014-2

A simple microfluidic device for the deformability assessment of blood cells in a continuous flow

Raquel O. Rodrigues[1,2] · **Diana Pinho**[2,3] · **Vera Faustino**[2,4] · **Rui Lima**[2,3,5]

Published online: 19 October 2015

Abstract Blood flow presents several interesting phenomena in microcirculation that can be used to develop microfluidic devices capable to promote blood cells separation and analysis in continuous flow. In the last decade there have been numerous microfluidic studies focused on the deformation of red blood cells (RBCs) flowing through geometries mimicking microvessels. In contrast, studies focusing on the deformation of white blood cells (WBCs) are scarce despite this phenomenon often happens in the microcirculation. In this work, we present a novel integrative microfluidic device able to perform continuous separation of a desired amount of blood cells, without clogging or jamming, and at the same time, capable to assess the deformation index (DI) of both WBCs and RBCs. To determine the DI of both WBCs and RBCs, a hyperbolic converging microchannel was used, as well as a suitable image analysis technique to measure the DIs of these blood cells along the regions of interest. The results show that the WBCs have a much lower deformability than RBCs when subjected to the same *in vitro* flow conditions, which is directly related to their cytoskeleton and nucleus contents. The proposed strategy can be easily transformed into a simple and inexpensive diagnostic microfluidic system to simultaneously separate and assess blood cells deformability.

Keywords Microfluidic devices · Cell separation and deformability · Hyperbolic microchannel · Blood on chips · RBC · WBC

Electronic supplementary material The online version of this article (doi:10.1007/s10544-015-0014-2) contains supplementary material, which is available to authorized users.

✉ Rui Lima
ruimec@ipb.pt

[1] LCM – Laboratory of Catalysis and Materials – Associate Laboratory LSRE/LCM, Faculdade de Engenharia, da Universidade do Porto (FEUP), R. Dr. Roberto Frias, 4200-465 Porto, Portugal

[2] Polytechnic Institute of Bragança, ESTiG/IPB, C. Sta. Apolónia, 5301-857 Bragança, Portugal

[3] CEFT, Faculdade de Engenharia da Universidade do Porto (FEUP), R. Dr. Roberto Frias, 4200-465 Porto, Portugal

[4] Center for MicroElectromechanical Systems (CMEMS-UMinho), University of Minho, Campus de Azurém, 4800-058 Guimarães, Portugal

[5] Mechanical Engineering Department, University of Minho, Campus de Azurém, 4800-058 Guimarães, Portugal

1 Introduction

Blood is an extremely information-rich and easily accessible tissue, which can be used to diagnose several diseases with multiple techniques. However, due to the complex blend of cells it requires the isolation of a limited number of cells, so an accurate analysis can be realized and eventually applied to a variety of biomedical applications, such as diagnostics, therapeutics and cell biology (Gossett et al. 2010). Most of the standard techniques used for cell separation and sorting are often labour intensive or require additional external labels to identify cells (Jinlong et al. 2008; Pinho et al. 2013). For these reasons, label-free microfluidic techniques have been raising interest, since they avoid the use of biochemical labels that may change the cell properties and increase costs (Gossett et al. 2010). Therefore, intrinsic biomarkers, such as cell size, electrical polarization, density, deformability and/or hydrodynamic properties are being explored (Chen et al. 2008; Hou et al. 2010; Kim et al. 2010; Pinho et al. 2013; Shevkoplyas et al. 2005). Concerning cells separation based on their size, microstructures such as micro-pillar arrays, micro-weir and membranes with holes have been used as a simple, non-

destructive and easy integrative step to be implemented, in order to archive a single and complete device (Bradley et al. 2012; Chen et al. 2008; Yang et al. 1999). Nevertheless, several separation microfluidic devices are based in dead-end filtration, which might lead to clogging or jamming (Agbangla et al. 2012; Chen et al. 2007; Georgieva et al. 2010). To overcome this issue, cross-flow filtration has being used (Tae Goo et al. 2014), operating under similar size-exclusion precepts, with the fluid flowing perpendicular to the micro-pillar arrays or micro-weir filters. Thereby, the rejected cells continue to travel in the direction of primary flow, while selected cells flow into a separated outlet (Chen et al. 2008; Gossett et al. 2010). Ji and his colleagues (Ji et al. 2008) have compared four main types of silicon-based microfilters and they have found that the cross-flow filtration approach is the most efficient way of sorting RBCs and WBCs. Additionally this microfilter was the most suitable for handling blood flow avoiding problems associated with aggregations of cells and filter clogging. Recently, some research works regarding the plasma separation from whole blood (Chen et al. 2008; VanDelinder and Groisman 2006), white blood cells (WBCs) from whole blood (VanDelinder and Groisman 2007), fluorescent polystyrene beads separated by sizes (Metz et al. 2004) and neonatal rat cardiac cell population from whole blood (Murthy et al. 2006) have been reported. However, to the best of our knowledge, no study has reported until now an integrative microfluidic device, capable of separating a small amount of blood cells (WBCs and red blood cells (RBCs)) from the initial blood fluid, and at the same time, studying and detecting changes in their deformability, through the deformation index (DI) assessment of isolated individual cells. In fact, in microfluidics and cell biology fields there is a need of a better understanding of the flow behaviour and deformation of WBCs in an *in vitro* environment. This type of environment was already shown to be very different from the *in vivo* ones, where WBCs adapt their shape (possibly by deformation) penetrating through the walls of vascular endothelial cells, by activation of pro-inflammatory mediators (cytokines, chemokines, or bacterial peptides) (Liu and Wang 2004). Since WBCs are a set of several types of different and specialized cells, they are usually subdivided in: granulocytes (neutrophils, basophils, and eosinophils), characterized by the presence of differently staining granules in their cytoplasm or agranulocytes (lymphocytes, monocytes, and macrophages), characterized by the apparent absence of granules in their cytoplasm (Khismatullin 2009). Due to the polymorphism and complexity of these cells, they should be studied individually, in order to verify their specificities of deformability and hydrodynamic properties, such as their sizes, cytoplasmatic contents and densities. In the group of agranulocytes, peripheral blood mononuclear cells (PBMC) (i.e., lymphocyte, monocyte or macrophage) are main actors in inflammatory processes and linked to many diseases, such as rheumatoid arthritis (Tanino et al. 2009), atherosclerosis (Ortega et al. 2012), asthma (Covar et al. 2010), HIV (Fu et al. 2011), cancer (Frampton et al. 2013), among others. Moreover, they are a potential source of non-invasive biomarkers for diagnosis and monitoring of many diseases (Maes et al. 2013). In this research, we develop a pillar-type cross-flow filtration microfluidic device to separate and collect RBCs and a specific type of WBCs, the PBMC, and then perform the individual deformation assessment of them, based on the extensional flow approach. The latter methodology was adopted due to the ability of providing a detailed quantitative description of the degree of deformation of blood cells under a controlled homogeneous extensional flow field, in a region of homogeneous extension rate. Studies focusing on the extensional flow effect on the blood cells deformability are scarce, despite this phenomenon often happens in the microcirculation, particularly when there is a sudden change in geometry and consequently, there is a dramatic change of the cells velocity and deformability. Recent studies performed by Lee et al. (2009), Yaginuma et al. (2013) and Faustino et al. (2014) have investigated RBCs behaviour under the effect of a extensional flow in hyperbolic converging microchannels. However, in the literature there are few studies concerning the effect of extensional-dominated flows on the deformation degree of WBCs. Therefore, the main purpose of this study is the development of an integrative microfluidic device able to separate from an initial *in vitro* blood sample, a low amount of blood cells (PBMCs and RBCs), and at the same time, evaluate their deformability through a hyperbolic converging microchannel.

2 Materials and methods

2.1 Microfluidic device design and fabrication

The microfluidic device used in the present work was designed to include a cross-flow filtration barrier to separate a low amount of WBCs (i.e., PBMCs) and RBCs from an *in vitro* blood sample, as well as several sequences of hyperbolic channels, in the outlet of the sub-channels, to perform deformability assessment on the separated blood cells. A schematic view of the microfluidic device with dimensions of the main channel, 55×500×17,482 μm (height × width × length), is shown in Fig. 1. The pillar-type filtration barrier was set with a total of 42 rectangular pillars with dimensions of 55× 50 μm (width × length), spaced by 10 μm, and the triplicate sequences of the hyperbolics were set in the outlet of the four sub-channels, with dimension of 55×20×383 μm (height × width × length). To perform the deformability assessment hyperbolic converging microchannels were designed with 382 μm of length, as well as widths of 400 and 20 μm at the wide and narrow sizes, respectively, corresponding to

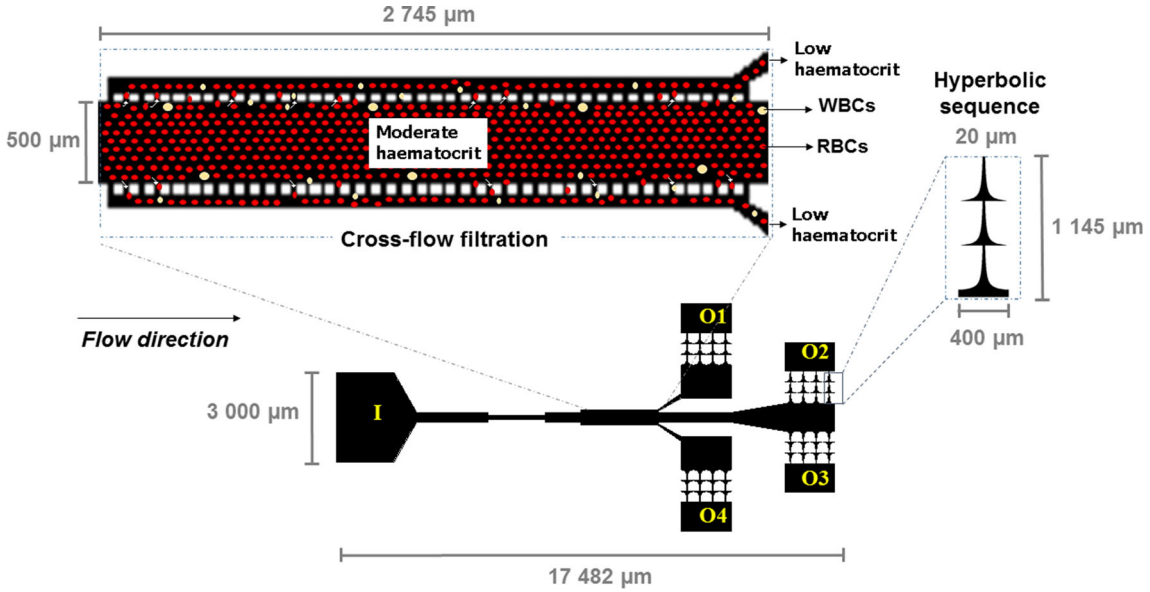

Fig. 1 Schematic view of the microfluidic device with zoom of the pillar-type filtration barrier to promote blood cells separation, as well as the hyperbolic sequence section to assess the deformation index of those blood cells. I, Inlet; O1, Outlet 1; O2, Outlet 2; O3, Outlet 3; O4, Outlet 4

hyperbolic contractions with a Hencky strain of~3. The polydimethylsiloxane (PDMS) microchannels were fabricated using soft lithographic technique from a mask-pattern fabricated by photolitography technique using photoresistant SU-8, as previously reported by Lima et al. (2008).

2.2 Working fluid protocol

The working fluid used in this study was Dextran 40 (Sigma-Aldrich, USA) solution containing 2 % of haematocrit (Hct 2 %, *v/v*) of RBCs and equal amount of PBMCs. PBMCs were collected from whole human blood by adapting the procedure described by Sigma-Aldrich® (Sigma-Aldrich 2011), with the commercial solution of Histopaque-1077 (Sigma-Aldrich, USA). Briefly, venous human blood samples from healthy donors were collected into 10 mL BD-Vacutainers (BD, USA) tubes containing ethylenediaminetetraacetic acid (EDTA). The whole blood was divided in two equal parts in order to obtain RBCs and PBMCs with the following procedures: (i) *RBCs collection*, 3 mL of whole blood was centrifuged immediately after collection at 2500 rpm for 10 min at 4 °C. After removing the buffy coat and plasma, the packed RBCs were re-suspended and washed twice in physiological salt solution (PSS) with 0.9 % NaCl (B. Braun Medical, Germany); (ii) *PBMCs collection*: 3 mL of whole blood was carefully added to 3 mL of Histopaque-1077 (Sigma-Aldrich, USA) at room temperature. After centrifuged for 30 min at 1900 rpm, the upper layer corresponding to plasma was discarded. Therefore, the opaque interface containing PBMCs was washed three times with 6 mL of Hank's Balanced Salt Solution without calcium or magnesium (HBSS, Life Technologies, USA) during 10 min at 1500 rpm, in order to remove possible contamination of platelets or RBCs. Then, the washed PBMCs were re-suspended in 1 mL of tissue culture medium, RPMI-1040 (Sigma-Aldrich, USA), and kept at 4 °C until being used in the experiments. Immediately before the experiments, the final working fluid was prepared by mixing together the collected RBCs and PBMCs in Dextran 40 solution (10 %, w/v). Dextran 40 is frequently used as substitute of the blood plasma, since it minimizes not only the sedimentation of the blood cells during the experimental assays but also cell clogging phenomenon.

2.3 Experimental set-up

The high-speed video microscopy system used in the present study consisted of an inverted microscope (IX71, Olympus) combined with a high-speed camera (Fastcam SA3, Photron, USA). The PDMS microchannel was placed and fixed in the microscope and the flow rate of the working fluids was kept constant at 100 µL/min by means of a syringe pump (PHD Ultra, Harvard Apparatus, USA) with a 5 mL syringe (Terumo, Japan). The fluids at the four outlets of the subchannels (O1, O2, O3 and O4) were collected into separated Eppendorfs to be further evaluated, concerning the cell separation efficiency, as shown in Fig. 2. At the same time, the images of the flowing cells at the established flow rate were captured by the high speed camera at a frame rate of 2000 frames/s and a shutter speed ratio of 1/75 000, which minimized the dragging of the cells at the high flow rate in study. All the experimental assays were performed at room temperature (T=22±1 °C).

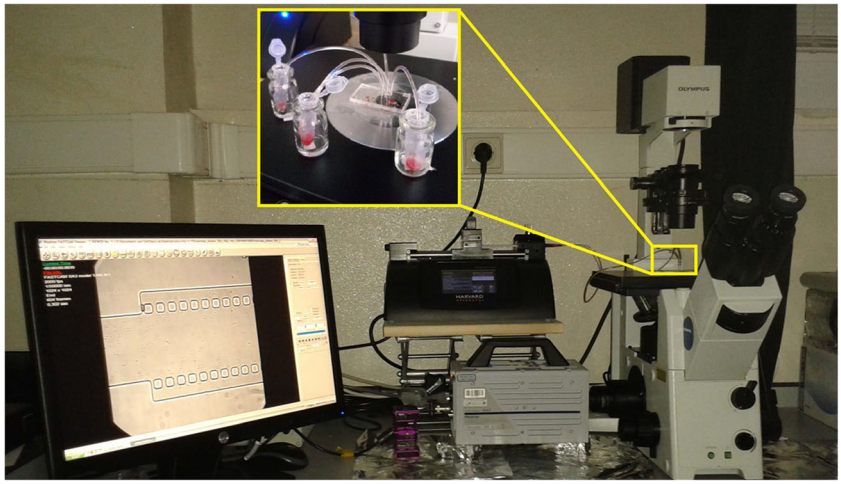

Fig. 2 Main experimental set-up used to perform the microfluidic tests

2.4 Determination of the blood cells separation

Individual Eppendorfs were placed close to the four outlets of the sub-channels, called as O1, O2, O3 and O4, allowing the collection, and further evaluation of the amount of blood cells that were separated by the cross-flow filtration barrier. Thus, an equal volume of 250 μL from each sub-channel was treated with RBCs lysis buffer (GBiosciences, USA) in a ratio of 1:2 (*v/v*), during 15 min at room temperature. This procedure enabled that only the RBCs were selectively lysed without affecting the viability of WBCs, and therefore, the PBMCs could be counted using a Neubauer chamber with accuracy. The method to count the PBMCs in a Neubauer chamber used in this work was the same as the recommended by Luttmann et al. (2006), where blood cells are counted within the four big squares of the Neubauer chamber. This procedure was performed in triplicate for each outlet and in two separated assays done in different days using the blood of two different healthy donors (n=6).

2.5 Image analysis

The experimental images recorded in each test were transferred to a computer, processed and analysed by an image handling software, ImageJ (1.46r, NIH, USA). Using this software, DI of the blood cells were calculated similarly as previously reported by Pinho et al. (2013). For all the measurements, major and minor axis lengths of the blood cells were used to determine RBCs and PBMCs DIs. The formula used to calculate the DI is presented as Eq. (1):

$$DI = \frac{(Lmajor - Lminor)}{(Lmajor + Lminor)} \quad (1)$$

where, L_{major} and L_{minor} refer to major and minor axis lengths of the blood cell, respectively.

For the assessment of the DI of each blood cells, 92 individual cells of RBCs and 76 PBMCs were randomly measured in the centre line position along the hyperbolic channel. Hence, a total of 168 individual blood cells were assessed to calculate the DI.

3 Results and discussion

3.1 Separation of blood cells in the microfluidic device

The main goal of this study is the development of a simple and integrative microfluidic device capable to perform at once and in continuous flow, the separation of a certain amount of blood cells from an initial *in vitro* blood sample, and simultaneously use the reduced amount of blood cells to perform their deformability assessment. Hence, this device can be a useful microfluidic tool, capable to assess and study the blood cells DIs, as they can be used as label-free biomarkers for the assessment of blood diseases. To gain insight in the deformability behavior of leukocyte cells, we have decided to investigate the PBMCs (i.e., lymphocyte, monocyte or macrophage), which are main actors in the inflammatory processes and linked to many blood diseases.

To achieve the best flow conditions to perform the microfluidic experimental assays, several experimental parameters had to be previously studied. One of the most critical parameter in all microfluidic tests is the choice of the most suitable flow rate that better fits on the purpose of the microfluidic study. Therefore, in order to evaluate the optimal flow rate for the better cell separation efficiency, a series of trial assays were previously made in the range between 10 and 200 μl/min. In these screening experiments, the blood cells (PBMCs and RBCs) were tracked at three representative positions (middle of the main channel, just above the pillars-wall and at the region between the middle position and pillars-wall)

at the cross-flow filtration region of the microchannel device (data not shown). To assess this data the manual tracking "MtrackJ" plugin (Meijering et al. 2006) from the image handling software, ImageJ (1.46r, NIH) was used to track PBMCs and RBCs, as similarly reported by Leble et al. (2011) and shown in Fig. 3 (more details in the supplementary video 1). Figure 3 shows clearly that the pillars provide a barrier to WBCs as a PBMC is rolling along the cross-flow pillars promoting this cell to flow within the main channel. In contrast, RBCs tend to deform and pass through the pillars into the branch channel.

As a result, the flow rate 100 μl/min was considered to be the most suitable to perform this study, due to the maintained flow stability, absence of clogging or jamming of the cells, as well as a better separation of the tracked blood cells along the cross-flow filtration channel. Therefore, this optimized flow rate allowed that just a small concentration of blood cells flow through the cross-flow pillar barrier, which promoted the optimum conditions to assess the individual cells DI. In contrast, the lower flow rates used in the screening experiments (10, 25 and 50 μl/min), often led to severe clogging and jamming of the blood cells. In particular, the PBMCs were often trapped within the pillars barrier with these lower flow rates, restricting the continuity of these assays and consequently compromising the assessment of the cells DIs. A possible explanation for these observed clogging and jamming phenomena is that at lower flow rates, stagnation regions where the cells velocity are close to zero, are more likely to happen around the cross-flow pillars. On the other hand, tests with higher flow rate, such as 200 μl/min, have resulted in high internal pressure and leakage of the working fluid. Note that high flow rates also increase the complexity of controlling the working fluid within the microchannel and measuring the deformability of the cells flowing through the hyperbolic contractions. Thus, according to these screening results, it was decided to select the flow rate of 100 μl/min, as the most suitable to perform our experimental tests.

Table 1 shows the amount of PBMCs cells/mL counted by means of a Neubauer chamber, as previously described in section 2.4., after the RBCs lysis treatment be applied into all the fluid samples collected at the four outlets.

The results shown in Table 1 demonstrate that even with a very simple cross-flow filtration geometry (consisting in just one linear sequence of square pillars), it is possible to obtain a desired amount of PBMCs for the further assessment of cells DI, which in this case represents about 25 % of cells from the initial working fluid. Figure 4 shows a representative illustration of the separation strategy and blood cells flowing through the pillar cross-flow barrier into the four outlets.

As it can be seen in Fig. 4, the combination of the cross-flow filtration with an optimal flow rate generates a cell-free layer in the lateral outlets promotes a decreasing on the total amount of blood cells flowing through that outlets. These decreasing of PBMCs in O1 and O4 were also qualitatively observed in the amount of RBCs. However, the qualitative data of the collected RBCs into these outlets had to be sacrificed in order to improve the accuracy of the counted PBMCs within the Neubauer chamber. As a result, the RBCs were lysed as previously described in the section 2.4., with minimal cellular effect on the WBCs.

3.2 Blood cells deformation assessment

In literature there are several published works regarding the correlation between RBCs, abnormal deformability and some diseases (e.g., malaria (Suwanarusk et al. 2004), diabetes (Sabo et al. 1993), coronary diseases (Yaylali et al. 2013), among others), showing the interest of this topic by several research groups. However, even though WBCs are known to be important cells, as they defend our body against bacteria, virus and other harmful agents, there are few works published in literature concerning the *in vitro* assessment of their deformability, motion and interaction with other blood cells in microfluidic devices. Therefore, in this study we measured the DI of both RBCs and WBCs (i.e., PBMCs) flowing through hyperbolic microchannels located downstream the cross-flow microfilters, designated as O1 and O4 (cf. Fig. 1). As described above, the cross-flow filtration used in this study has promoted the reduction of the concentration of both

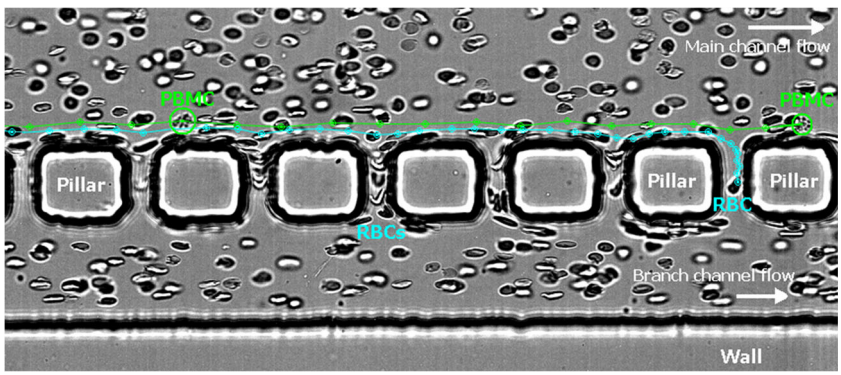

Fig. 3 Trajectories of both RBC and PBMC flowing around the pillars. The PBMC rolls along the pillars in the direction of primary flow whereas the RBC deforms and pass through the narrow gap between the pillars into the branch channel (see also supplementary video 1)

Table 1 Separation results of the PBMCs in continuous flow rate at 100 μL/min using a simple cross-flow filtration microdevice

Microdevice section	PBMCs±SD (10^4 cells/mL)	PBMCs (%)
Outlet 1	19±4.8	22
Outlet 2,3	46±7.9	52
Outlet 4	22±6.0	26

Results are presented as Mean±Standard Deviation (10^4 cells/mL) and in percentage (%) (n=6)

PBMC Peripheral blood mononuclear cells

WBCs and RBCs passing to the outlets O1 and O4 (as shown in Table 1 and Fig. 4). This low concentration was appropriate to obtain video images with single individual blood cells. However, this is not the case of the hyperbolic channels located around the outlets O2 and O3, where the high concentration of cells does not allow to accurately perform deformability assessment of individual blood cells.

After the cells concentration be decreased from the initial *in vitro* blood sample, due to the cross-flow filtration, the initial flow rate was slightly reduced with the presence of reservoirs located immediately before of each hyperbolic sequences in the four outlets of the microfluidic device (cf. Fig. 1). These geometries allowed that the DI assessment of the blood cells could be made by means of our high speed video camera, with minimal dragging of the cells.

Figure 5 shows the DIs of the blood cells (RBCs and PBMCs) flowing along the axial position of a hyperbolic channel with a sudden expansion, as well as the average or pseudo shear rate, $\overline{\gamma} = \frac{U}{D_h}$, at each hyperbolic region, where U is the mean velocity of the blood cells obtained at each region and D_h is the hydraulic diameter of each microchannel section.

Overall, the DI of both cells has a maximum value at the region right before the exit of the contraction, where the average shear rate is also the highest (1761.6 s^{-1}). In fact, the maximum average shear rate obtained at the narrowest region is in good agreement with the shear rate values encountered in arterioles (~1600 s^{-1}), which have dimensions similar to the hyperbolic contractions used in this work (~ 20 μm) (Papaioannou and Stefanadis 2005). After the narrowest section, cells tend to recover to its initial shape that corresponds to a minimal value of the DI, where cells are no longer exposed to extensional flow and the average shear rate reduces to extremely low value (60.7 s^{-1}), similarly to the values encountered at large veins. Moreover, the shear stress encountered in the arterioles (shear rate ~1600 s^{-1}) is around 55 dyn/cm^2 and this value decreases to 5 dyn/cm^2 at large veins, where the shear rate is~100 s^{-1} (Papaioannou and Stefanadis 2005). Therefore, our results show that both shear and extensional flows generated by the hyperbolic channels promote cell response to shear stress in a similar way that happens in *in vivo* environments.

Figure 5 also shows the difference between the DI obtained by the RBCs and PBMCs when exposed to the same strong extensional flow and shear stress conditions. It should be noted that the hyperbolic contraction geometry to measure the cells deformability with a Hencky strain of~3 was chosen mainly due to the strong extensional flow generated in the middle of the microchannel, which is dominant over the shear flow. To better understand the influence of the extensional flow and shear stress on the deformability of both RBCs and PBMCs, average DI values at the two key regions of the microchannel (narrow and recuperation section) were selected and defined as section 1 and 2 (Fig. 6).

The first DI measurement was made in the hyperbolic constriction section (section 1) that promotes the elongation of the cells caused by the strong extensional and shear flow (Lee et al. 2009; Yaginuma et al. 2013). The second DI assessment was measured in the recovery section caused by the sudden expansion (section 2), where the recovery to the normal size and shape of the blood cells can be seen. These two DIs assessment provided a better understanding of the deformation phenomenon by showing the different behaviour that blood cells have when subjected to the same strong extensional flow and high shear rate (section 1) and then the recovery of their initial shape, which

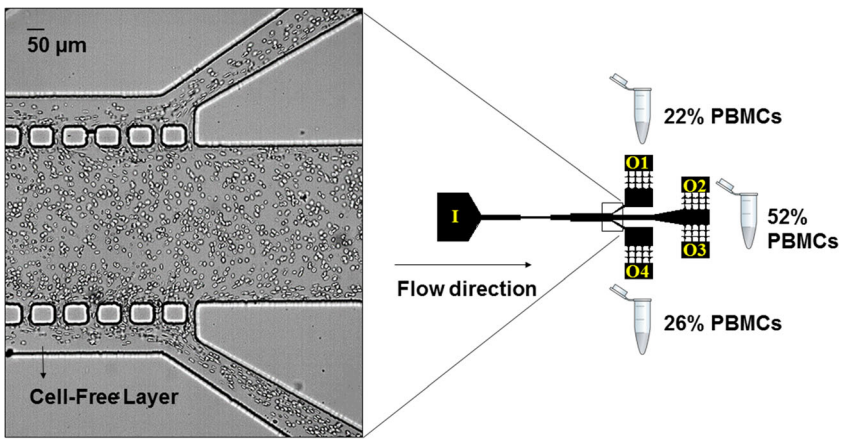

Fig. 4 Blood cells flowing through cross-flow filtration barrier to the direction of the outlets and hyperbolic chamber for their further DI assessment

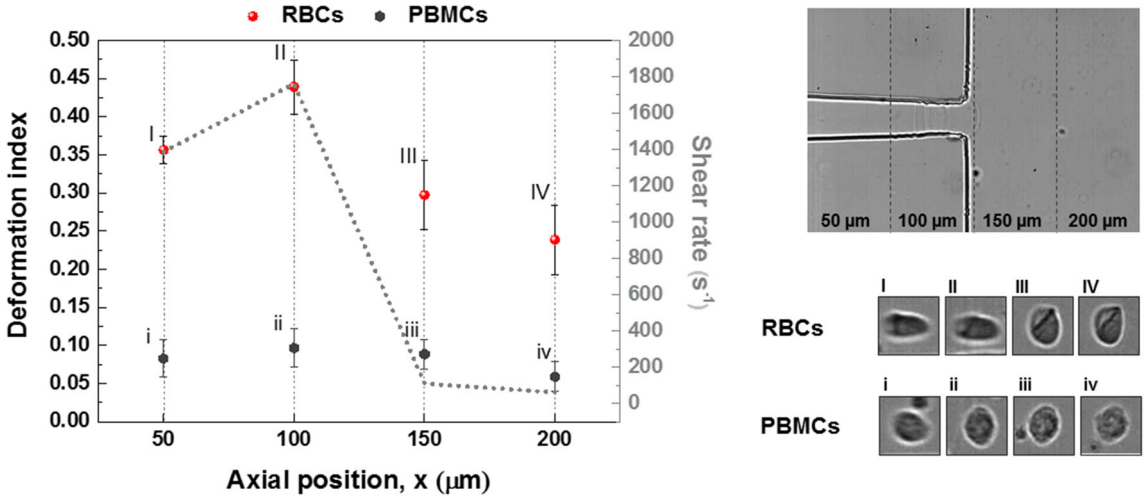

Fig. 5 Deformation index of blood cell (RBCs and PBMCs) flowing along the axial position of the hyperbolic channel followed by a sudden expansion (*red and black dots*), as well as the average shear rate at each hyperbolic region (*dotted line*). *Error bars* shows a 95 % of confidence interval (n=168 blood cells)

corresponds to a minimal value of the DI, where cells are no longer exposed to these deformable hemodynamic conditions (section 2). The results show that PBMCs, when submitted to a strong extensional flow and high flow rate, can reach a maximum DI of 0.10, followed by a small decrease of the DI to about 0.06, in the recovery section (n=76). It is worth mentioning that similar results were obtained by Gossett et al. (2012), regarding the deformation of untreated PBMCs subjected to a stretching extensional flow in a microfluidic deformability cytometer. By calculating the DI in the same way that Gossett et al. (2012) (length of the longer axis divided by the perpendicular of the shorter axis), our results shown a mean deformation of PBMCs about 1.21±0.13 (n=76), which is in good agreement with the data obtained by Gossett et al. (2012) where the mean deformation of these blood cells were calculated to be 1.18 (n=377). These results reveal that PBMCs under the applied *in vitro* conditions tend to behave as a non-deformed cell, indicating the importance of the pro-inflammatory mediators (cytokines, chemokines or bacterial peptides) have into the deformation of these cells, as observed in *in vivo* (Liu and Wang 2004) for the active WBCs deformation. Additionally, the results show the importance of the leukocyte-endothelial cell interaction, which is intimately linked to the cytoskeleton structures of the WBCs (namely the microvilli projections of them) and the nucleus content (e.g., cytoplasm viscosity). In fact, the cytoskeleton structure and internal composition of the WBCs are the main reasons for the rolling and arrest (firm adhesion) phenomena that allows their capture from the blood flow by the endothelial cells and further migration of these blood cells to search for bacteria or fungi through the body (Khismatullin 2009). These phenomena (specially the rolling) were also observed in this study along the whole microfluidic device (either in the cross-flow pillars, as shown in Fig. 3 and supplementary video 1, and in the hyperbolic channels), which we believe is the main reason for the difference of blood cells contents (WBCs and RBCs) that we have observed in the four outlets, as well as for the lower deformability observed in the hyperbolic channel, when compared with the RBCs DIs. Moreover, Fig. 6 shows that the RBCs, when submitted to the same strong extensional flow and high shear rate, tend to elongate (especially when they travel along the centreline of the hyperbolic section), reaching a maximum DI of 0.44±0.04, which corresponds fourfold higher than the deformability reached by PBMCs. Also, it can be observed in this figure that this high RBC deformability is followed by a dramatic decrease of their DI to 0.24±0.05. This latter result corroborate with the ones obtained by Lee et al. (2009) and Yaginuma et al. (2013), where they found that RBCs change

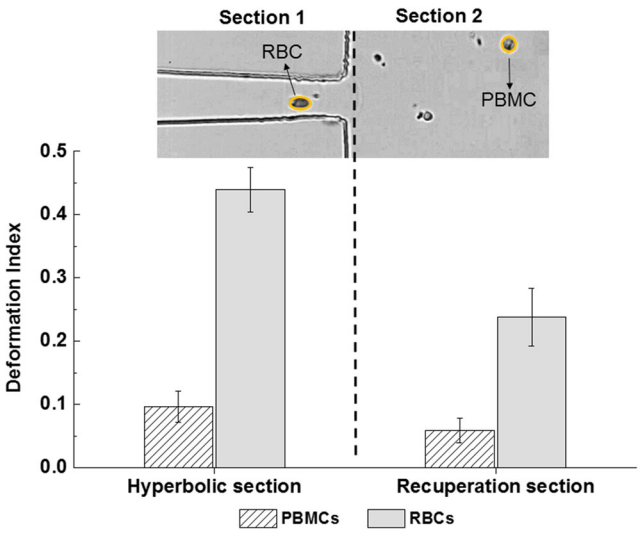

Fig. 6 Averaged deformation index obtained from PBMCs and RBCs flowing within the hyperbolic and recuperation section of the microchannel device. Error bars shows a 95 % of confidence interval (n=168)

from a nearly circular to an elliptical shape and become increasingly elongated as they flow through a hyperbolic contraction. Hence, the results obtained by this study indicate that RBCs under *in vitro* and passive hemodynamic conditions, presents higher deformability behaviour when compared to the PBMCs deformability results. Since the WBCs are naturally known as deformable cells in their biological environment, this paradoxical *in vitro* results corroborated the fact that Gossett et al. (2012) pointed to the relevance of pro-inflammatory mediators in the activation of the deformation behaviour of these blood cells, as well as for the importance to study the mechanical properties of each type of WBCs when subjected to passive deformability. Additionally, these *in vitro* hemodynamic behaviours encountered among different blood cells may have the potential to become a new μTAS able to use these findings to improve the separation of different blood cells from the whole blood based on their natural and passive hydrodynamic behaviour, and therefore, eventually, allowing the development of a simple and disposable clinical microfluidic system.

4 Conclusions

In this work we have successfully designed, fabricated and tested a novel microfluidic device able to perform continuously and simultaneously both separation of a certain amount of blood cells from an initial blood sample, as well as to assess the deformability of them, by using respectively, cross-flow microfilters and hyperbolic microchannels. The cross-flow filtration strategy has shown the ability to separate from the initial *in vitro* blood sample, approximately 25 % of PBMCs and to collect directly to the two outlets located downstream of this barrier. This separation efficiency was proven to be the most adequate way to assess blood cells deformability by using our high-speed video microscopy system. The major advantage of this separation technique was the ability to investigate, for the first time, the effect of extensional-dominated flows on the deformability of both PBMCs and RBCs under the same *in vitro* conditions using hyperbolic chambers. The DI results have shown that PBMCs have a non-deformable behaviour when subjected to passive hemodynamic conditions even with a strong extensional flows, which is in good agreement with the recently published study performed by Gossett et al. (2012). In contrast, RBCs have shown to have a much higher deformable behaviour when subjected to the same *in vitro* conditions (fourfold higher than the deformability reached by PBMCs). Although there are many advantages with the proposed microfluidic device, including its low cost, ease of fabrication and cell separation simplicity, its biggest challenges are its ability to perform whole blood cells separation without any problems of clogging or jamming and the need to use a high-speed video microscopy system to measure the cells deformability. Further improvements in the proposed microfluidic design and the integration of optical components within the device are expected to lead to the creation of a novel μTAS for routine cell screening in clinical and research applications.

Acknowledgments The authors acknowledge the financial support provided by PTDC/SAU-ENB/116929/2010 and EXPL/EMS-SIS/2215/2013 from FCT (Fundação para a Ciência e a Tecnologia), COMPETE, QREN and European Union (FEDER). R. O. Rodrigues, D. Pinho and V. Faustino acknowledge respectively, the PhD scholarships SFRH/BD/97658/2013, SFRH/BD/89077/2012 and SFRH/BD/99696/2014 granted by FCT. The authors would also like to thank Dr. Ângela Fernandes for providing the blood samples and Dr. Ricardo Calhelha for supplying the tissue culture medium used in this work.

References

G.C. Agbangla, É. Climent, P. Bacchin, Sep. Purif. Technol. **101**, 42–48 (2012)
E.L. Bradley, L. Bernard, P. Thomas, J. Brian, J. Micromech. Microeng. **22**, 025009 (2012)
X. Chen, D. Cui, C. Liu, H. Li, J. Chen, Anal. Chim. Acta **584**, 237–243 (2007)
X. Chen, D.F. Cui, C.C. Liu, H. Li, Sens. Actuators B Chem. **130**, 216–221 (2008)
R. Covar, M. Gleason, B. Macomber, L. Stewart, P. Szefler, K. Engelhardt, J. Murphy, A. Liu, S. Wood, S. DeMichele, E.W. Gelfand, S.J. Szefler, Clin. Exp. Allergy **40**, 1163–1174 (2010)
V. Faustino, D. Pinho, T. Yaginuma, R. Calhelha, I.F.R. Ferreira, R. Lima, BioChip J. **8**, 42–47 (2014)
A.E. Frampton, C.E. Fletcher, T.M. Gall, L. Castellano, C.L. Bevan, J. Stebbing, J. Krell, Expert. Rev. Mol. Diagn. **13**, 425–430 (2013)
J. Fu, B.E. Sha, L.L. Thomas, J. Acquir. Immune Defic. Syndr. **56**, 16–25 (2011)
K. Georgieva, D.J. Dijkstra, H. Fricke, N. Willenbacher, J. Colloid Interface Sci. **352**, 265–277 (2010)
D.R. Gossett, W.M. Weaver, A.J. Mach, S.C. Hur, H.T. Tse, W. Lee, H. Amini, D. Di Carlo, Anal. Bioanal. Chem. **397**, 3249–3267 (2010)
D.R. Gossett, H.T.K. Tse, S.A. Lee, Y. Ying, A.G. Lindgren, O.O. Yang, J. Rao, A.T. Clark, D. Di Carlo, Proc. Natl. Acad. Sci. U. S. A. **109**, 7630–7635 (2012)
H.W. Hou, A.A. Bhagat, A.G. Chong, P. Mao, K.S. Tan, J. Han, C.T. Lim, Lab Chip **10**, 2605–2613 (2010)
H.M. Ji, V. Samper, Y. Chen, C.K. Heng, T.M. Lim, L. Yobas, Biomed. Microdevices **10**, 251–257 (2008)
Z. Jinlong, G. Qiuquan, L. Mei, Y. Jun, J. Micromech. Microeng. **18**, 125025 (2008)
D.B. Khismatullin, in *Leukocyte rolling and adhesion: Current topics in membranes*, ed. by K. Ley, vol. 64 (Academic, New York, 2009), pp. 47–111
M. Kim, S. Mo Jung, K.H. Lee, Y. Jun Kang, S. Yang, Artif. Organs **34**, 996–1002 (2010)
V. Leble, R. Lima, R. Dias, C. Fernandes, T. Ishikawa, Y. Imai, T. Yamaguchi, Biomicrofluidics **5**, 044120-044120-044115 (2011)
S. Lee, Y. Yim, K. Ahn, S. Lee, Biomed. Microdevices **11**, 1021–1027 (2009)
R. Lima, S. Wada, S. Tanaka, M. Takeda, T. Ishikawa, K. Tsubota, Y. Imai, T. Yamaguchi, Biomed. Microdevices **10**, 153–167 (2008)
X.H. Liu, X. Wang, J. Biomech. **37**, 1079–1085 (2004)
W. Luttmann, K. Bratke, M. Kupper, D. Myrtek, *Immunology*, vol. 1 (Elsevier, Philadelphia, 2006)
E. Maes, B. Landuyt, I. Mertens, L. Schoofs, PLoS One **8**, e61933 (2013)

E. Meijering, I. Smal, G. Danuser, IEEE Signal Process. Mag. **23**, 46–53 (2006)

S. Metz, C. Trautmann, A. Bertsch, R. Ph, J. Micromech. Microeng. **14**, 324 (2004)

S.K. Murthy, P. Sethu, G. Vunjak-Novakovic, M. Toner, M. Radisic, Biomed. Microdevices **8**, 231–237 (2006)

E. Ortega, R. Gilabert, I. Nuñez, M. Cofán, A. Sala-Vila, E. de Groot, E. Ros, Atherosclerosis **221**, 275–281 (2012)

T.G. Papaioannou, C. Stefanadis, Hellenic J. Cardiol. **46**, 9–15 (2005)

D. Pinho, T. Yaginuma, R. Lima, BioChip J. **7**, 367–374 (2013)

A. Sabo, V. Jakovljevic, M. Stanulovic, L. Lepsanovic, D. Pejin, Int. J. Clin. Pharmacol. Ther. Toxicol. **31**, 1–5 (1993)

S.S. Shevkoplyas, T. Yoshida, L.L. Munn, M.W. Bitensky, Anal. Chem. **77**, 933–937 (2005)

Sigma-Aldrich, Histopaque-1077: product information. St. Louis, MO, USA, (2011)

R. Suwanarusk, B.M. Cooke, A.M. Dondorp, K. Silamut, J. Sattabongkot, N.J. White, R. Udomsangpetch, J. Infect. Dis. **189**, 190–194 (2004)

K. Tae Goo, Y. Yong-Jin, J. Hongmiao, L. Pei Yi, C. Yu, J. Micromech. Microeng. **24**, 087001 (2014)

M. Tanino, R. Matoba, S. Nakamura, H. Kameda, K. Amano, T. Okayama, H. Nagasawa, K. Suzuki, K. Matsubara, T. Takeuchi, Biochem. Biophys. Res. Commun. **387**, 261–265 (2009)

V. VanDelinder, A. Groisman, Anal. Chem. **78**, 3765–3771 (2006)

V. VanDelinder, A. Groisman, Anal. Chem. **79**, 2023–2030 (2007)

T. Yaginuma, M.S.N. Oliveira, R. Lima, T. Ishikawa, T. Yamaguchi, Biomicrofluidics **7**, 054110 (2013)

X. Yang, J.M. Yang, Y.-C. Tai, C.-M. Ho, Sensors Actuators A Phys. **73**, 184–191 (1999)

Y.T. Yaylali, I. Susam, E. Demir, M. Bor-Kucukatay, B. Uludag, E. Kilic-Toprak, G. Erken, D. Dursunoglu, J. Coron. Artery Dis. **24**, 11–15 (2013)